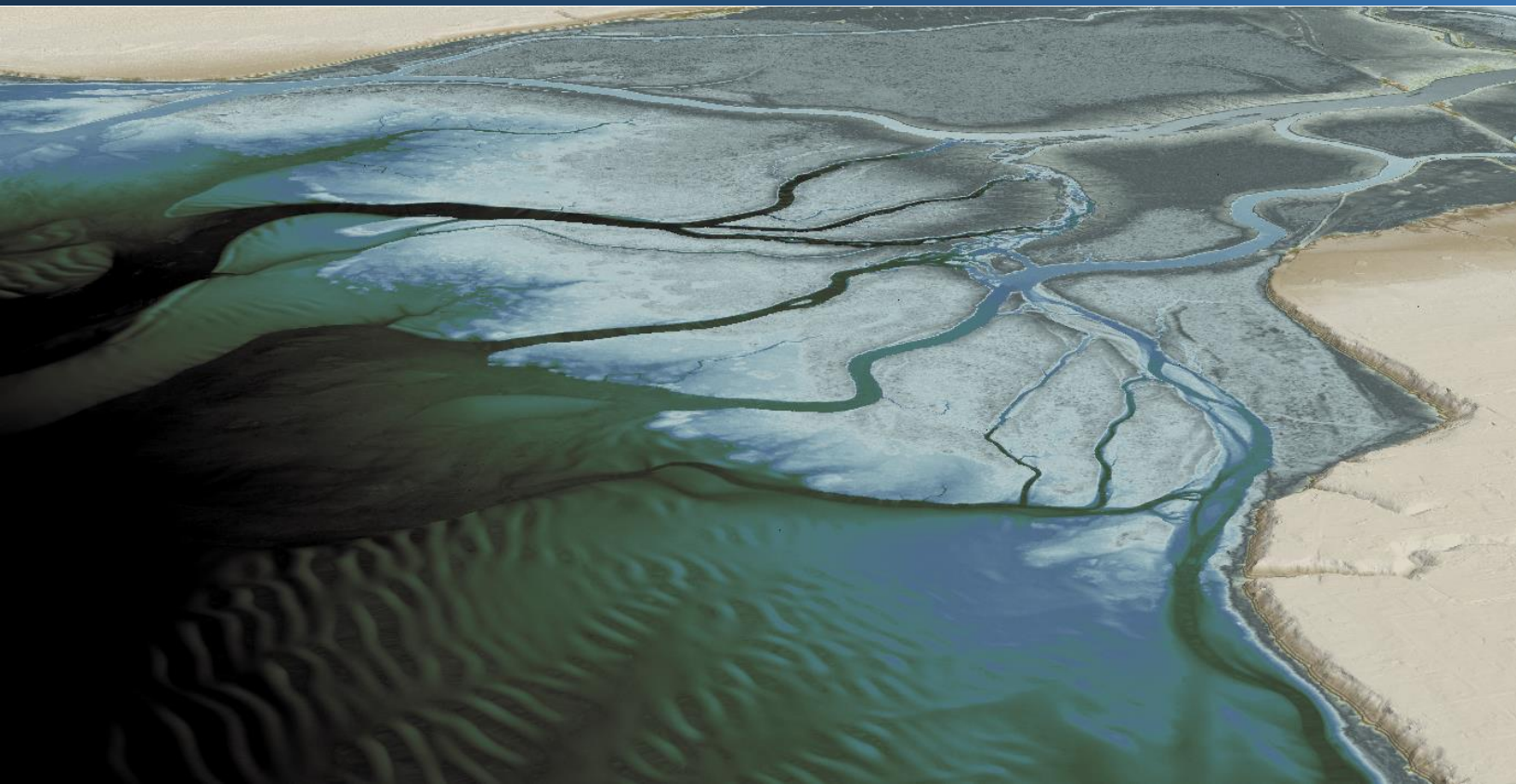




Applied
Remote Sensing
and Analysis

July 26, 2013



Nooksack River Basin LiDAR

Technical Data Report – Delivery 2



Treva Coe
Nooksack Indian Tribe
P.O. Box 157
5016 Deming Rd.
Demming, WA 98244
PH: 360.592.5176



Diana Martinez
PSRC
1011 Western Ave.
Suite 500
Seattle, WA 98104
PH: 206.971.3052



WSI Corvallis Office
517 SW 2nd St., Suite 400
Corvallis, OR 97333
PH: 541-752-1204

TABLE OF CONTENTS

- INTRODUCTION 1
- ACQUISITION 4
 - Planning..... 4
 - Ground Survey..... 5
 - Monumentation 5
 - RTK Surveys..... 6
 - Airborne LiDAR Survey 8
- PROCESSING 9
 - LiDAR Data..... 9
- RESULTS & DISCUSSION 11
 - LiDAR Density 11
 - LiDAR Accuracy Assessments 15
 - LiDAR Absolute Vertical Accuracy..... 15
 - LiDAR Relative Vertical Accuracy 16
- CERTIFICATIONS 17
- SELECTED IMAGES..... 18
- GLOSSARY 23
- APPENDIX A - ACCURACY CONTROLS 24

Cover Photo: Confluence of the Nooksack River and the Pacific Ocean, the bare-earth model is colored by elevation.

INTRODUCTION

View of the Nooksack River in northwest Washington showing the mixed conifer landscape



In July 2012, WSI (Watershed Sciences, Inc.) was contracted by the Nooksack Indian Tribe and the Puget Sound LiDAR Consortium (PSLC) to collect Light Detection and Ranging (LiDAR) data on a 5-year cycle for the Nooksack River Basin LiDAR site in Northwest Washington. Data were collected to aid the Tribe in assessing the topographic and geophysical properties of the study area to support restoration efforts.

This data delivery and report covers the entire project area, including the portion of the Middle Fork Nooksack River which was delayed due to snow conditions. It describes the LiDAR data and documents data acquisition procedures, processing methods, and results of all accuracy assessments. Project specifics are shown in Table 1, the project extent can be seen in Figure 1, and a complete list of contracted deliverables provided to PSLC and the Tribe can be found in Table 2.

Table 1: Acquisition dates, acreages, and data types collected on the Nooksack River Basin LiDAR site

Project Site	Contracted Acres	Buffered Acres	Acquisition Dates	Data Type	Delivery Date
Delivery 1: Mainstem North Fork & South Fork Nooksack	108,386	116,490	1/12/2013	LiDAR	6/17/2013
			1/13/2013		
			1/15/2013		
			3/31/2013		
Delivery 2: Full project area including Middle Fork Nooksack			4/1/2013		7/26/2013
			4/3/2013		
			4/15/2013		
			6/16/2013		
			6/28/2013		

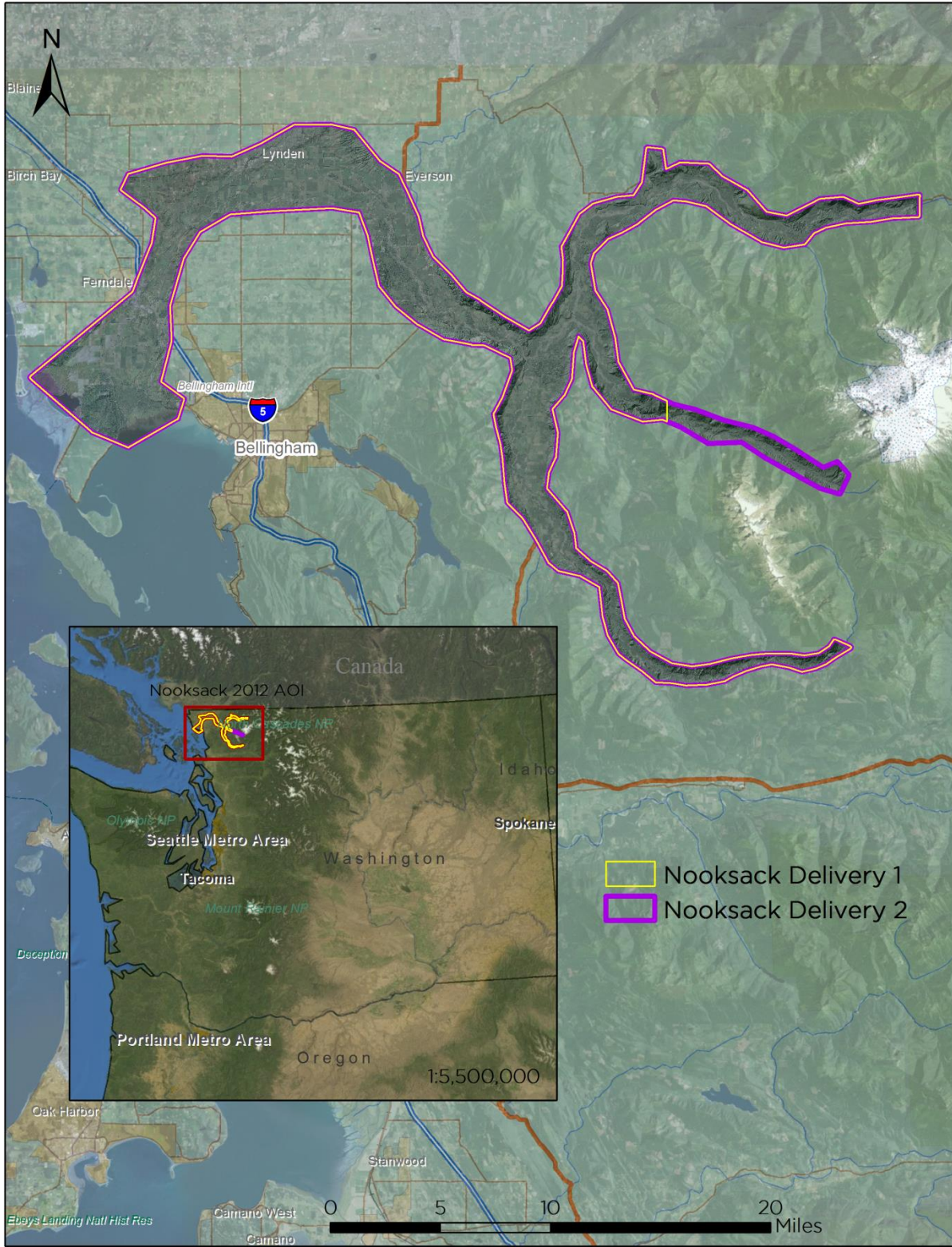


Figure 1: Location map of the Nooksack River Basin LiDAR site in northwest Washington

Table 2: Products delivered to PSLC

Nooksack River Basin LiDAR Products Projection: Washington State Plane North FIPS 4601 Horizontal Datum: NAD83 (CORS96)** Vertical Datum: NAVD88 (GEOID03) Units: U.S. Survey Feet	
LAS Files	LAS v 1.2 <ul style="list-style-type: none"> • All Returns Text Files (*.txt) <ul style="list-style-type: none"> • All Returns • Ground Returns
Rasters	3-foot ESRI Grids <ul style="list-style-type: none"> • Bare Earth Model • Highest Hit Model 1.5-foot GeoTiffs <ul style="list-style-type: none"> • Intensity Images
Vectors	Shapefiles (*.shp) <ul style="list-style-type: none"> • Site Boundary • LiDAR Index • DEM/DSM Index • Smooth Best Estimate Trajectory (SBETs) • Ground Control Points Text Files (*.txt) <ul style="list-style-type: none"> • Smooth Best Estimate Trajectory (SBETs)

defined as NAD83 (HARN) for GIS purposes



WSI Cessna Caravan



Planning

In preparation for data collection, WSI reviewed the project area using Google Earth, and flightlines were developed using a combination of specialized software. Careful planning by acquisition staff entailed adapting the pulse rate, flight altitude, scan angle, and ground speed to ensure complete coverage of the study area at the target point density of ≥ 8 pulses per square meter (0.74 pulses/square foot). Efforts are taken to optimize flight paths by minimizing flight times while meeting all accuracy specifications.

Factors such as satellite constellation availability and weather windows must be considered during the planning stage. Any weather hazards or conditions affecting the flight were continuously monitored due to their potential impact on the daily success of airborne and ground operations. In addition, a variety of logistical considerations required review including private property access, potential air space restrictions, and availability of company resources (both staff and equipment).

Special care was taken to acquire the tidal flats at low tide where possible. Acquisition on the upper reach of the Middle Fork Nooksack study area was postponed due to snow. Full acquisition of the entire area was completed on July 28, 2013.

Ground Survey

Ground survey data is used to geospatially correct the aircraft positional coordinate data and to perform quality assurance checks on final LiDAR data. Ground professionals set permanent survey monuments and collect real time kinematic (RTK) surveys to support the airborne LiDAR acquisition process.



Monumentation

The spatial configuration of ground survey monuments provided redundant control within 13 nautical miles of the mission areas for LiDAR flights. Monuments were also used for collection of ground control points using RTK survey techniques (see **RTK** below).

Monument locations were selected with consideration for satellite visibility, field crew safety, and optimal location for RTK coverage. WSI utilized 1 existing monument from a previous Nooksack acquisition (NF_NOOK_01) and established 10 new monuments for the project (Table 3, Figure 2). New monumentation was set using 5/8"x30" rebar topped with stamped 2" aluminum caps. WSI's professional land surveyor, Chris Yotter-Brown (WAPLS#46328 LS) oversaw and certified the establishment of all monuments.

Table 3: Monuments established for the Nooksack River Basin LiDAR acquisition. Coordinates are on the NAD83 (CORS96) datum, epoch 2002.00.

Monument ID	Latitude	Longitude	Ellipsoid (meters)
NF_NOOK_01	48° 53' 34.32858"	-121° 57' 54.54998"	248.903
NF_NOOK_02_RESET	48° 54' 34.23945"	-121° 47' 54.74509"	554.099
NOOK_06	48° 53' 16.20241"	-122° 32' 22.33185"	-2.096
NOOK_07	48° 50' 01.79580"	-122° 36' 22.88766"	-16.584
NOOK_08	48° 54' 20.41755"	-122° 19' 30.42889"	8.555
NOOK_09	48° 56' 03.97273"	-122° 21' 13.56824"	2.864
NOOK_10	48° 50' 26.36404"	-122° 08' 55.21014"	72.151
NOOK_11	48° 44' 45.75110"	-122° 11' 44.64782"	60.099
NOOK_12*	48° 41' 08.70523"	-122° 11' 29.81193"	76.423
NOOK_12_RES	48° 41' 08.70507"	-122° 11' 29.81218"	76.421
NOOK_13	48° 41' 15.60676"	-122° 10' 28.62599"	85.586

*NOOK_12 was discovered destroyed between acquisition days and was replaced with NOOK_12_RES.

To correct the continuous onboard measurements of the aircraft position recorded throughout the missions, WSI concurrently conducted multiple static Global Navigation Satellite System (GNSS) ground surveys (1 Hz recording frequency) over each monument. After the airborne survey, the static GPS data were triangulated with nearby Continuously Operating Reference Stations (CORS) using the Online

Positioning User Service (OPUS¹) for precise positioning. Multiple independent sessions over the same monument were processed to confirm antenna height measurements and to refine position accuracy.

Monuments were established according to the national standard for geodetic control networks, as specified in the Federal Geographic Data Committee Draft Geospatial Position Accuracy Standards, Part 2, Table 2.1 (FGDC-STD-007.2-1998). This standard provides guidelines for classification of monument quality at the 95% confidence interval as a basis for comparing the quality of one control network to another. The monument rating for this project can be seen in Table 4.

Table 4: Federal Geographic Data Committee monument rating

Direction	Rating
St Dev _{NE} :	0.050 m
St Dev _z :	0.050 m

For the Nooksack River Basin LiDAR project, the monument positions contributed no more than 5 cm of horizontal and vertical error to the final RTK and LiDAR positions, with 95% confidence.

RTK Surveys

For the real time kinetic (RTK) check point data collection, Trimble R7 and R8 base units were positioned at a nearby monument to broadcast a kinematic correction to a roving Trimble R6 or R10 receiver. All RTK measurements were made during periods with a Position Dilution of Precision (PDOP) of ≤ 3.0 with at least six satellites in view of the stationary and roving receivers. When collecting RTK data, the rover would record data while stationary for five seconds, then calculate the pseudorange position using at least three one-second epochs. Relative errors for the position must be less than 1.5 cm horizontal and 2.0 cm vertical in order to be accepted. See Table 5 for Trimble unit specifications.

RTK positions were collected on paved roads and other hard surface locations such as gravel or stable dirt roads that also had good satellite visibility. RTK measurements were not taken on highly reflective surfaces such as center line stripes or lane markings on roads due to the increased noise seen in the laser returns over these surfaces. The distribution of RTK points depended on ground access constraints and may not be equitably distributed throughout the study area. See Figure 2 for the distribution of RTK in this project.

¹ OPUS is a free service provided by the National Geodetic Survey to process corrected monument positions. <http://www.ngs.noaa.gov/OPUS>.

Table 5: Trimble equipment identification

Receiver Model	Antenna	OPUS Antenna ID	Use
Trimble R6	Integrated GNSS Antenna R6	TRM_R6	RTK
Trimble R7 GNSS	Zephyr GNSS Geodetic Model 2	TRM57971.00	Static
Trimble R8	Integrated Antenna R8 Model 2	TRM_R8_GNSS	RTK/Static
Trimble R10	Integrated Antenna R10	TRMR10	RTK

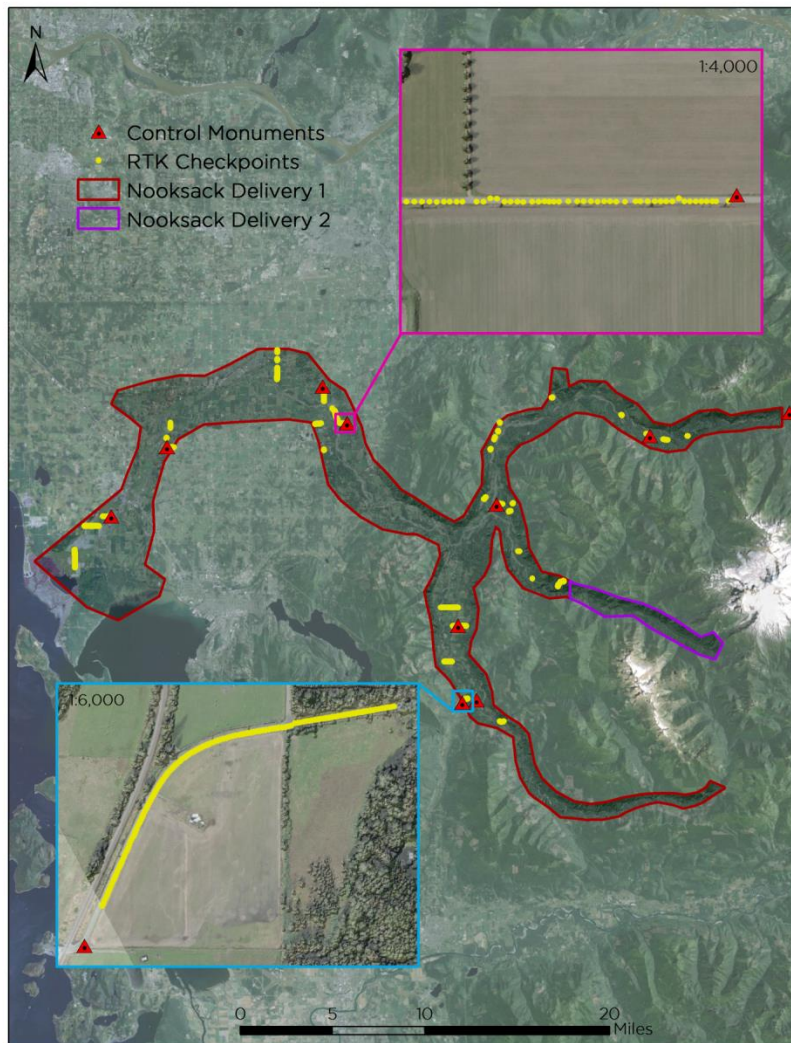


Figure 2: Basestation and RTK checkpoint location map

Airborne LiDAR Survey

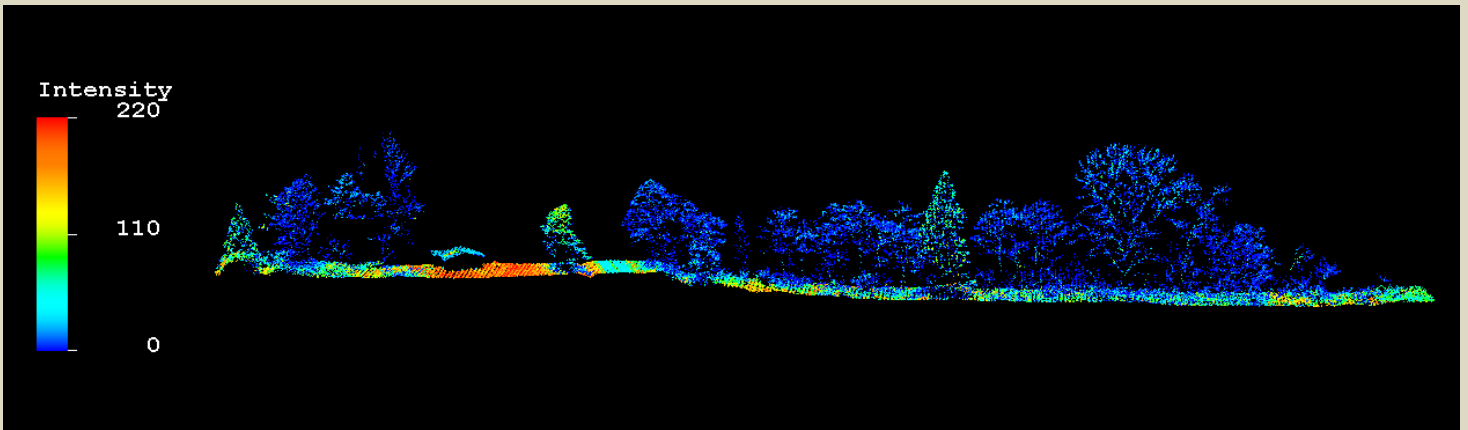
The LiDAR survey was accomplished with both a Leica ALS50 Phase II and a Leica ALS60 system independently mounted in Cessna Caravans. Table 6 summarizes the settings used to yield an average pulse density of ≥ 8 pulses/m² over the Nooksack River Basin LiDAR terrain. Specifications are shown by date. It is not uncommon for some types of surfaces (e.g. dense vegetation or water) to return fewer pulses to the LiDAR sensor than the laser originally emitted. These discrepancies between native and delivered density will vary depending on terrain, land cover, and the prevalence of water bodies.

Table 6: LiDAR specifications and survey settings

LiDAR Survey Settings & Specifications			
Survey Dates	1/12/2013 1/13/2013	1/15/2013	3/31/2013 4/1/2013 4/3/2013 4/16/2013 6/16/2013 6/28/2013
Sensor	Leica ALS60	Leica ALS60	Leica ALS50
Survey Altitude (AGL)	1500 m	900 m	900 m
Target Pulse Rate	148.8 kHz	105.9 kHz	105.9 kHz
Sensor Configuration	Single Pulse in Air (SPiA)	SPiA	SPiA
Laser Pulse Diameter	34 cm	21 cm	21 cm
Mirror Scan Rate	63.3 Hz	63.3 Hz	54.0 Hz
Field of View	24°	28°	28°
GPS Baselines	≤ 13 nm	≤ 13 nm	≤ 13 nm
GPS PDOP	≤ 3.0	≤ 3.0	≤ 3.0
GPS Satellite Constellation	≥ 6	≥ 6	≥ 6
Maximum Returns	4	4	4
Intensity	8-bit	8-bit	8-bit
Resolution/Density	Average 8 pulses/m ²	Average 8 pulses/m ²	Average 8 pulses/m ²
Accuracy	RMSE _z ≤ 15 cm	RMSE _z ≤ 15 cm	RMSE _z ≤ 15 cm

To reduce laser shadowing and increase surface laser painting, all areas were surveyed with an opposing flight line side-lap of $\geq 50\%$ ($\geq 100\%$ overlap). The Leica laser systems record up to four range measurements (returns) per pulse. All discernible laser returns were processed for the output dataset.

To accurately solve for laser point position (geographic coordinates x, y, z), the positional coordinates of the airborne sensor and the attitude of the aircraft were recorded continuously throughout the LiDAR data collection mission. Position of the aircraft was measured twice per second (2 Hz) by an onboard differential GPS unit. Aircraft attitude was measured 200 times per second (200 Hz) as pitch, roll, and yaw (heading) from an onboard inertial measurement unit (IMU). To allow for post-processing correction and calibration, aircraft/sensor position and attitude data are indexed by GPS time.



LiDAR Data

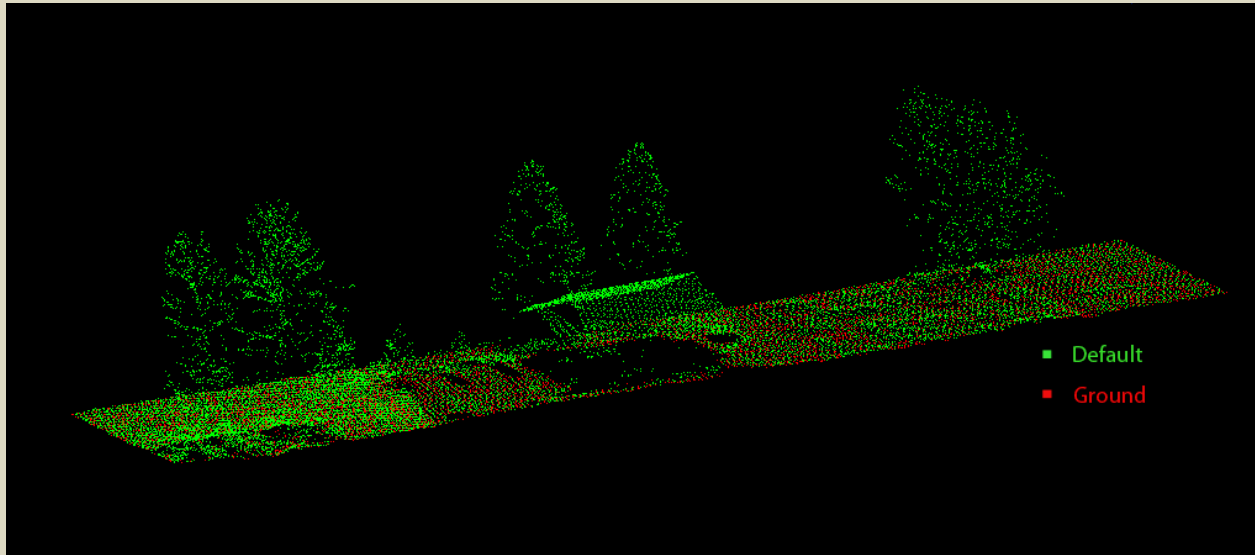
Upon the LiDAR data's arrival to the office, WSI processing staff initiates a suite of automated and manual techniques to process the data into the requested deliverables. Processing tasks include GPS control computations, smoothed best estimate trajectory (SBET) calculations, kinematic corrections, calculation of laser point position, calibration for optimal relative and absolute accuracy, and classification of ground and non-ground points (Table 7). Processing methodologies are tailored for the landscape and intended application of the point data. A full description of these tasks can be found in Table 8.

Table 7: ASPRS LAS classification standards applied to the Nooksack River Basin LiDAR dataset

Classification Number	Classification Name	Classification Description
1	Default/ Unclassified	Laser returns that are not included in the ground class and not dismissed as Noise or Withheld points
2	Ground	Ground that is determined by a number of automated and manual cleaning algorithms to determine the best ground model the data can support

Table 8: LiDAR processing workflow

LiDAR Processing Step	Software Used
Resolve kinematic corrections for aircraft position data using kinematic aircraft GPS and static ground GPS data.	Waypoint GPS v.8.3 Trimble Business Center v.3.00 Geographic Calculator 2013
Develop a smoothed best estimate of trajectory (SBET) file that blends post-processed aircraft position with attitude data. Sensor head position and attitude are calculated throughout the survey. The SBET data are used extensively for laser point processing.	IPAS TC v.3.1
Calculate laser point position by associating SBET position to each laser point return time, scan angle, intensity, etc. Create raw laser point cloud data for the entire survey in *.las (ASPRS v. 1.2) format. Data are converted to orthometric elevations (NAVD88) by applying a Geoid12 correction.	ALS Post Processing Software v.2.74
Import raw laser points into manageable blocks (less than 500 MB) to perform manual relative accuracy calibration and filter erroneous points. Ground points are then classified for individual flight lines (to be used for relative accuracy testing and calibration).	TerraScan v.13.008
Using ground classified points per each flight line, the relative accuracy is tested. Automated line-to-line calibrations are then performed for system attitude parameters (pitch, roll, heading), mirror flex (scale) and GPS/IMU drift. Calibrations are calculated on ground classified points from paired flight lines and results are applied to all points in a flight line. Every flight line is used for relative accuracy calibration.	TerraMatch v.13.002
Classify resulting data to ground and other client designated ASPRS classifications (Table 7). Assess statistical absolute accuracy via direct comparisons of ground classified points to ground RTK survey data.	TerraScan v.13.008 TerraModeler v.13.002
Generate bare earth models as triangulated surfaces. Highest hit models were created as a surface expression of all classified points (excluding the noise and withheld classes). All surface models were exported as ESRI grids at a 3-foot pixel resolution.	TerraScan v.13.008 ArcMap v. 10.1 TerraModeler v.13.002



LiDAR Density

The sensor is set to acquire a native density of 8 points/m² (0.74 points/ft²). Depending on the nature of the terrain, the first returned echo will be the highest hit surface. In vegetated areas, the first return surface will represent the top of the canopy, while in clearings or on paved roads, the first return surface will represent the ground. The ground density differs from the first return density due to the fact that in vegetated areas, fewer returns may penetrate the canopy. The ground classification is generally determined by first echo returns in non-vegetated areas combined with last echo returns in vegetated areas. The pulse density distribution will vary within the study area due to laser scan pattern and flight conditions. Additionally, some types of surfaces (i.e. breaks in terrain, water, steep slopes) may return fewer pulses to the sensor than originally emitted by the laser.

The average first-return density for the LiDAR data for the Nooksack River Basin LiDAR was 0.87 points/ft² (9.40 points/m²) (Table 9). The statistical distribution of first returns (Figure 3) and classified ground points (Figure 4) are portrayed below. Also presented are the spatial distribution of average first return densities (Figure 5) and ground point densities (Figure 6) for each 100mx100m cell.

Table 9: Average LiDAR point densities

Classification	Point Density
First-Return	0.87 points/ft ²
	9.40 points/m ²
Ground Classified	0.20 points/ft ²
	2.13 points/m ²

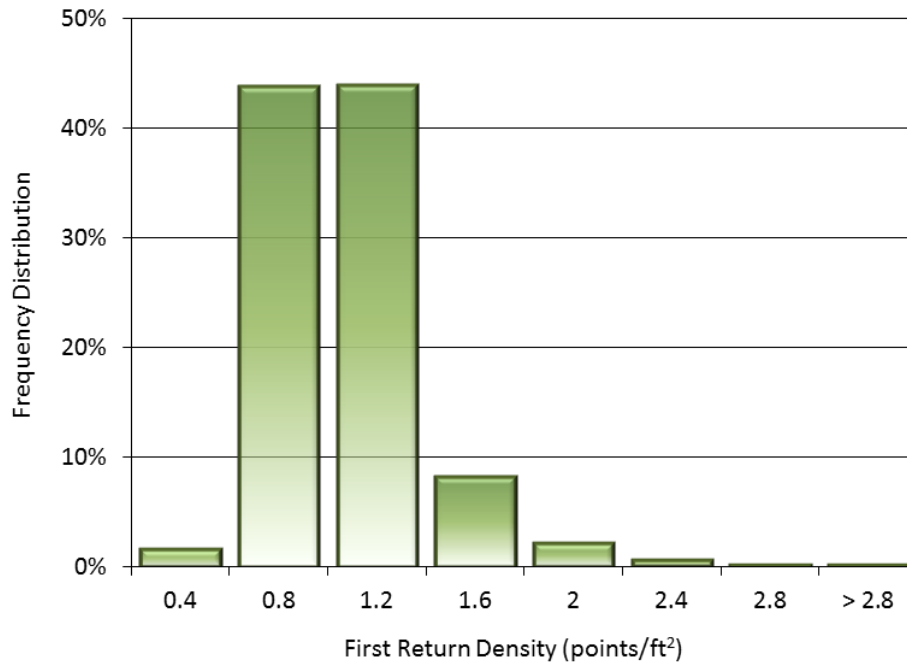


Figure 3: Frequency distribution of first return densities (native densities) of the gridded study area

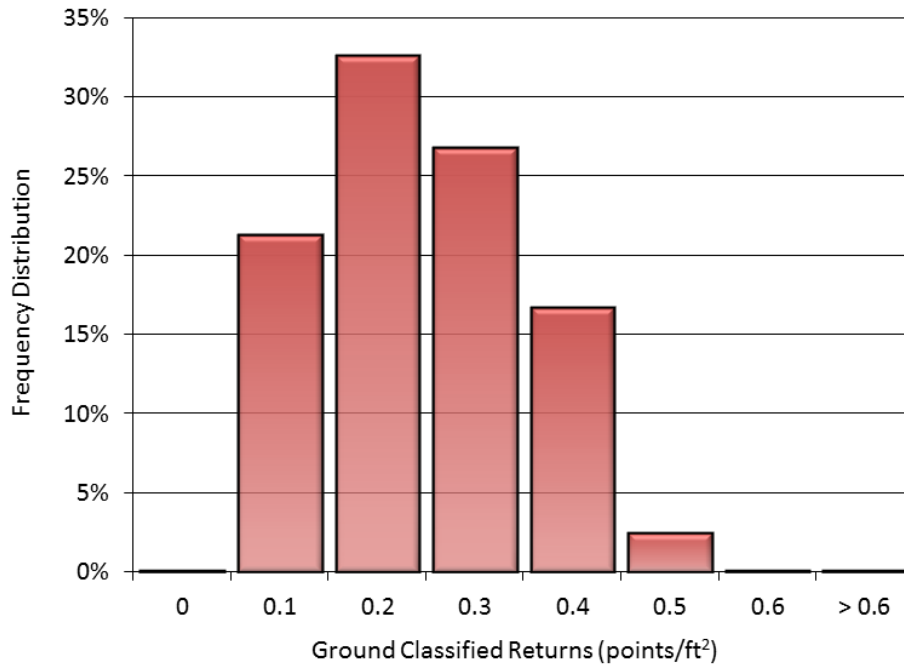


Figure 4: Frequency distribution of ground return densities of the gridded study area

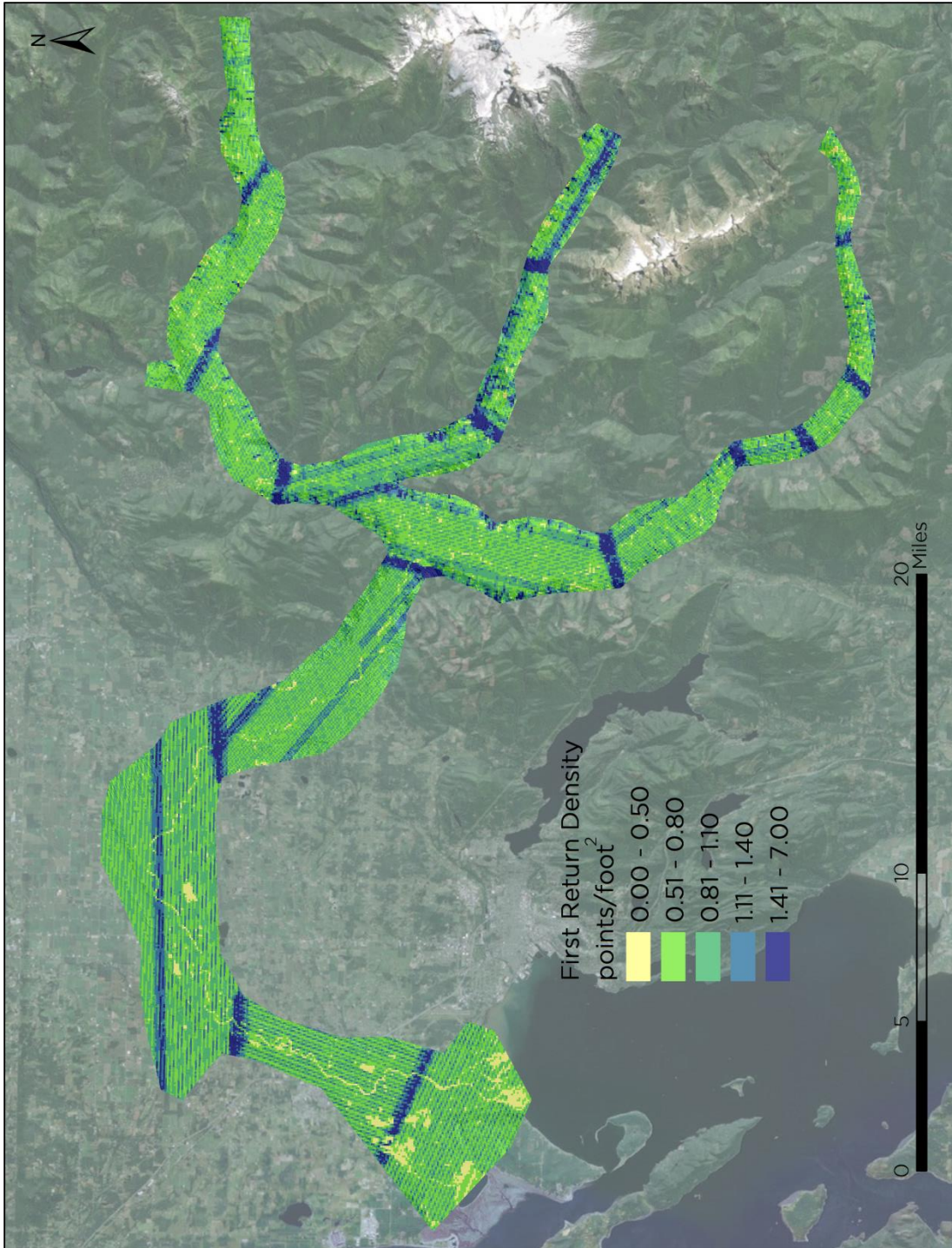


Figure 5: Native density map for the Nooksack River Basin LiDAR site (100mx100m cells)

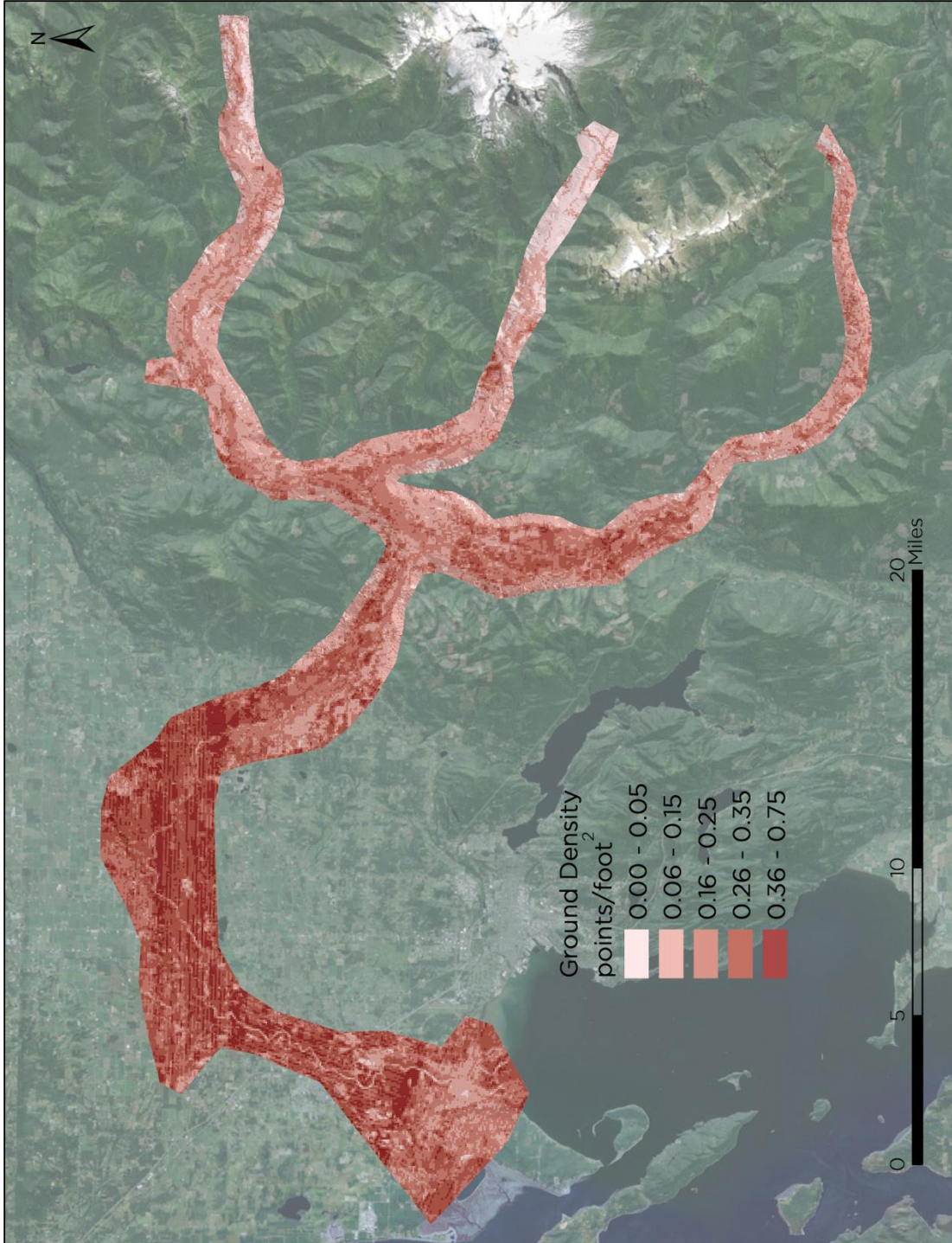


Figure 6: Ground density map for the Nooksack River Basin LiDAR site (100mx100m cells)

LiDAR Accuracy Assessments

The accuracy of the LiDAR data collection can be described in terms of absolute accuracy (the consistency of the data with external data sources) and relative accuracy (the consistency of the dataset with itself). See Appendix A for further information on sources of error and operational measures used to improve relative accuracy.

LiDAR Absolute Vertical Accuracy

Vertical absolute accuracy was primarily assessed from RTK ground check point (GCP) data collected on open, bare earth surfaces with level slope (<20°). Fundamental Vertical Accuracy (FVA) reporting is designed to meet guidelines presented in the National Standard for Spatial Data Accuracy (FGDC, 1998). FVA compares known RTK ground survey check points to the triangulated ground surface generated by the LiDAR points. FVA is a measure of the accuracy of LiDAR point data in open areas where the LiDAR system has a “very high probability” of measuring the ground surface and is evaluated at the 95% confidence interval (1.96 σ).

Absolute accuracy is described as the mean and standard deviation (sigma σ) of divergence of the ground surface model from ground survey point coordinates. These statistics assume the error for x, y, and z is normally distributed, and therefore the skew and kurtosis of distributions are also considered when evaluating error statistics. For the Nooksack River Basin LiDAR survey, 2,344 RTK points were collected in total resulting in an average accuracy of -0.011 feet (-0.003 meters) (Table 10, Figure 7).

Table 10: Absolute and relative vertical accuracies

	Absolute Accuracy	Relative Accuracy
Sample	2,344 points	383 surfaces
Average	-0.011 ft	0.098 ft
	-0.003 m	0.030 m
Median	-0.003 ft	0.130 ft
	-0.001 m	0.040 m
RMSE	0.076 ft	0.146 ft
	0.023 m	0.045 m
1σ	0.075 ft	0.056 ft
	0.023 m	0.017 m
2σ	0.148 ft	0.110 ft
	0.045 m	0.034 m

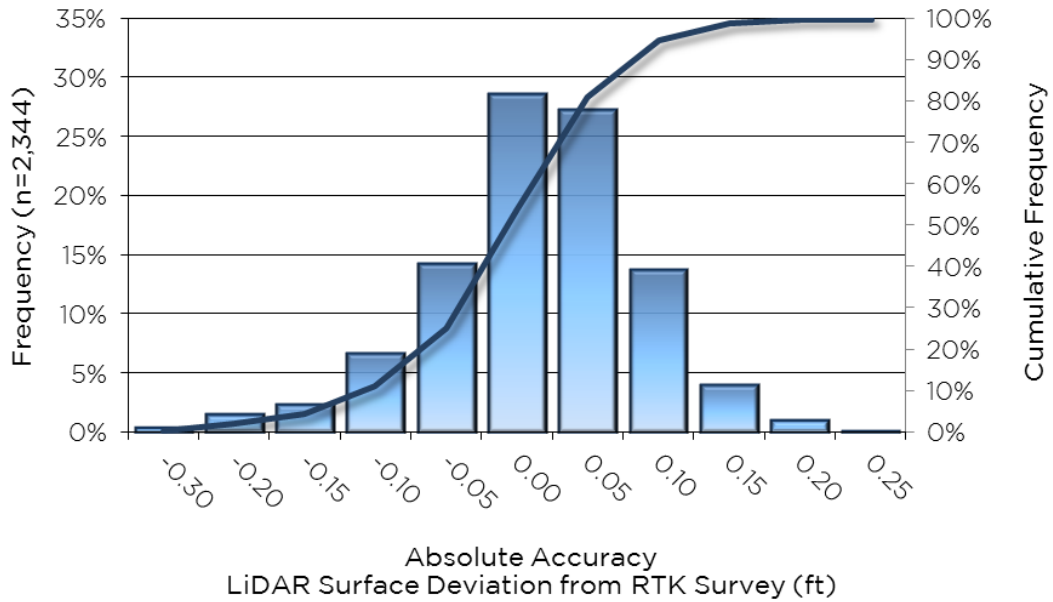


Figure 7: Frequency histogram for LiDAR surface deviation from RTK values

LiDAR Relative Vertical Accuracy

Relative vertical accuracy refers to the internal consistency of the data set as a whole: the ability to place an object in the same elevation given multiple flight lines, GPS conditions, and aircraft attitudes. When the LiDAR system is well calibrated, the swath-to-swath vertical divergence is low (<0.10 meters). The relative vertical accuracy is computed by comparing the ground surface model of each individual flight line with its neighbors in overlapping regions. The average line to line relative vertical accuracy for the entire Nooksack River Basin LiDAR area was 0.098 feet (0.030 meters) (Table 10, Figure 8).

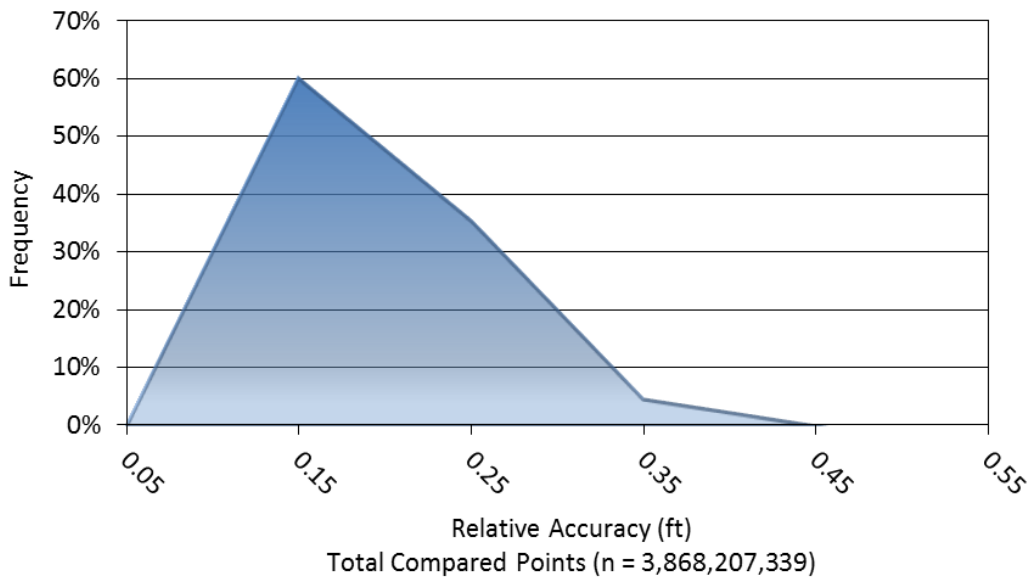


Figure 8: Frequency plot for relative accuracy between flight lines

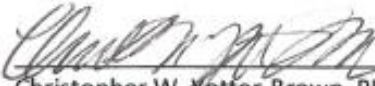
CERTIFICATIONS

Watershed Sciences provided LiDAR services for the Nooksack River Basin study area as described in this report.

I, Russ Faux, have reviewed the attached report for completeness and hereby state that it is a complete and accurate report of this project.

Russ Faux
Principal
WSI

I, Christopher W. Yotter-Brown, being first dully sworn, say that as described in the Ground Survey subsection of the Acquisition section of this report was completed by me or under my direct supervision and was completed using commonly accepted standard practices. Accuracy statistics shown in the Accuracy Section have been reviewed by me to meet National Standard for Spatial Data Accuracy.

 6/17/2013
Christopher W. Yotter-Brown, PLS Oregon & Washington
WSI
Portland, OR 97204



Renews: 12/21/2014

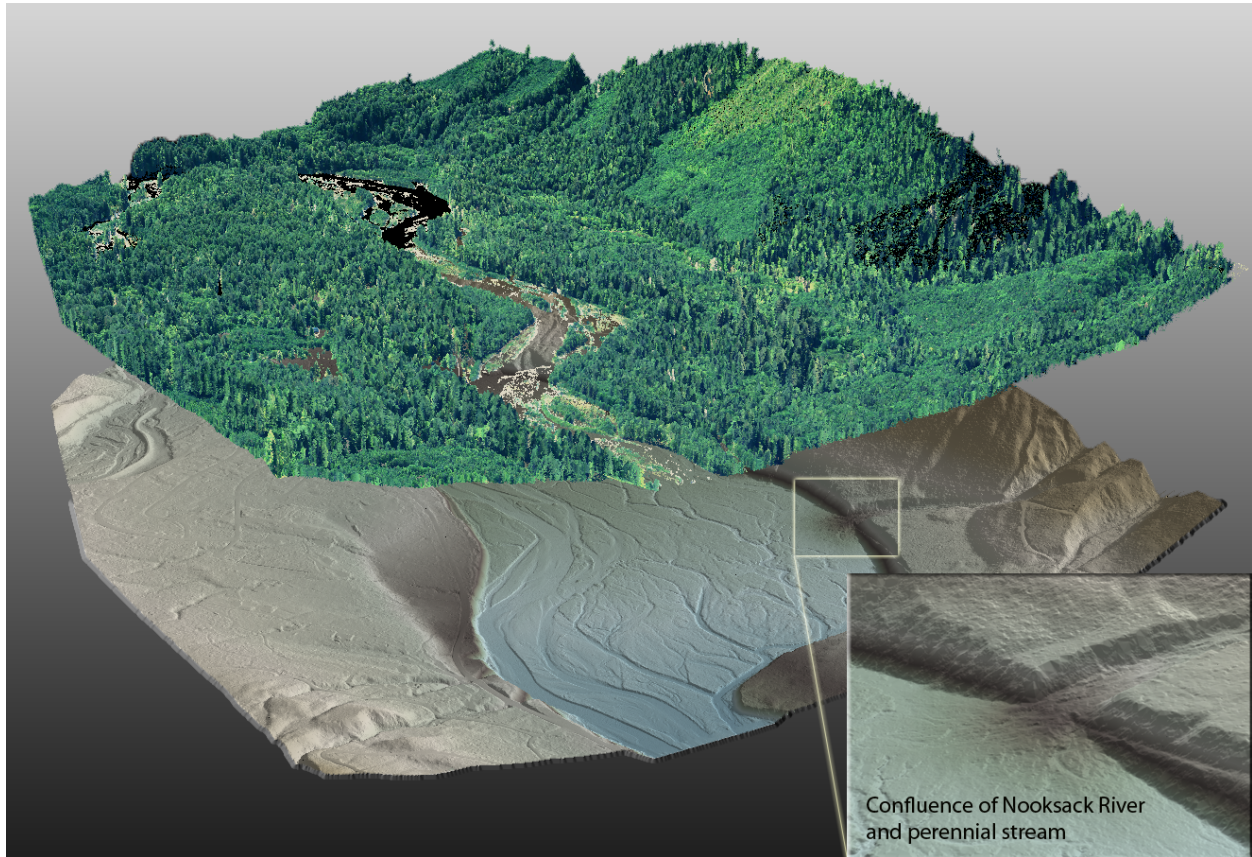


Figure 9: Layered view of Nooksack River along route 542. The scene demonstrates the ability of the laser to penetrate dense vegetation to reveal subtle terrain morphology. The top image is the LiDAR point cloud colored by NAIP and the bottom image is the gridded, bare-earth model colored by elevation.

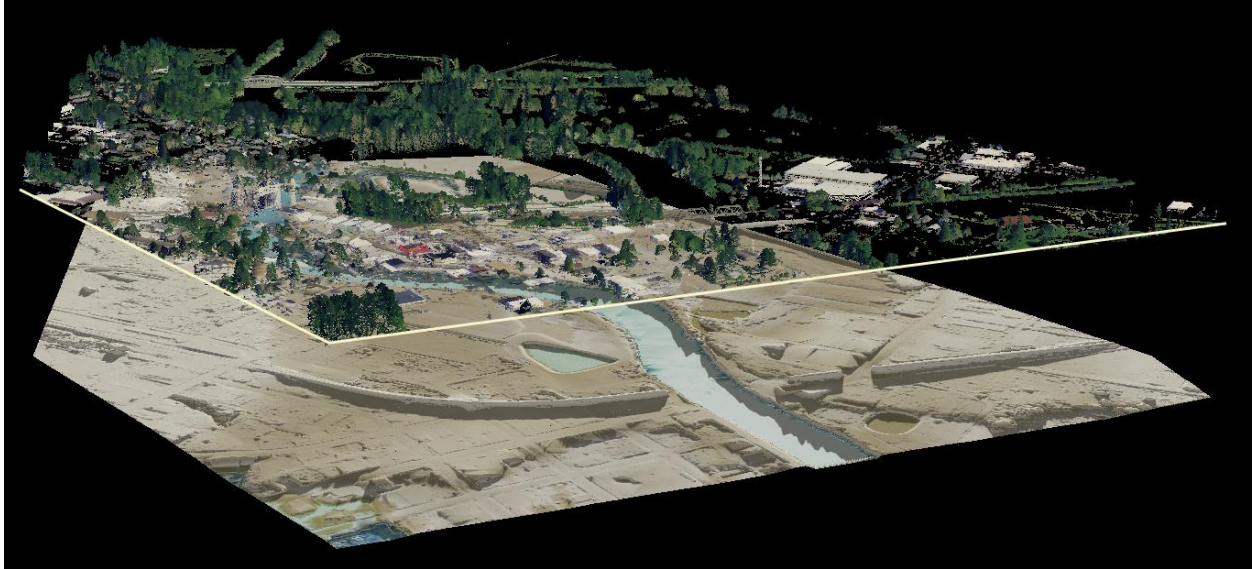


Figure 10: Layered view of the Nooksack River. The bottom image is the gridded, bare-earth surface colored by elevation; the top image is the LiDAR point cloud with ground classified returns removed.



Figure 11: Close up view looking at the estuary at the mouth of the Nooksack River. Image created from bare-earth LiDAR model colored by elevation.

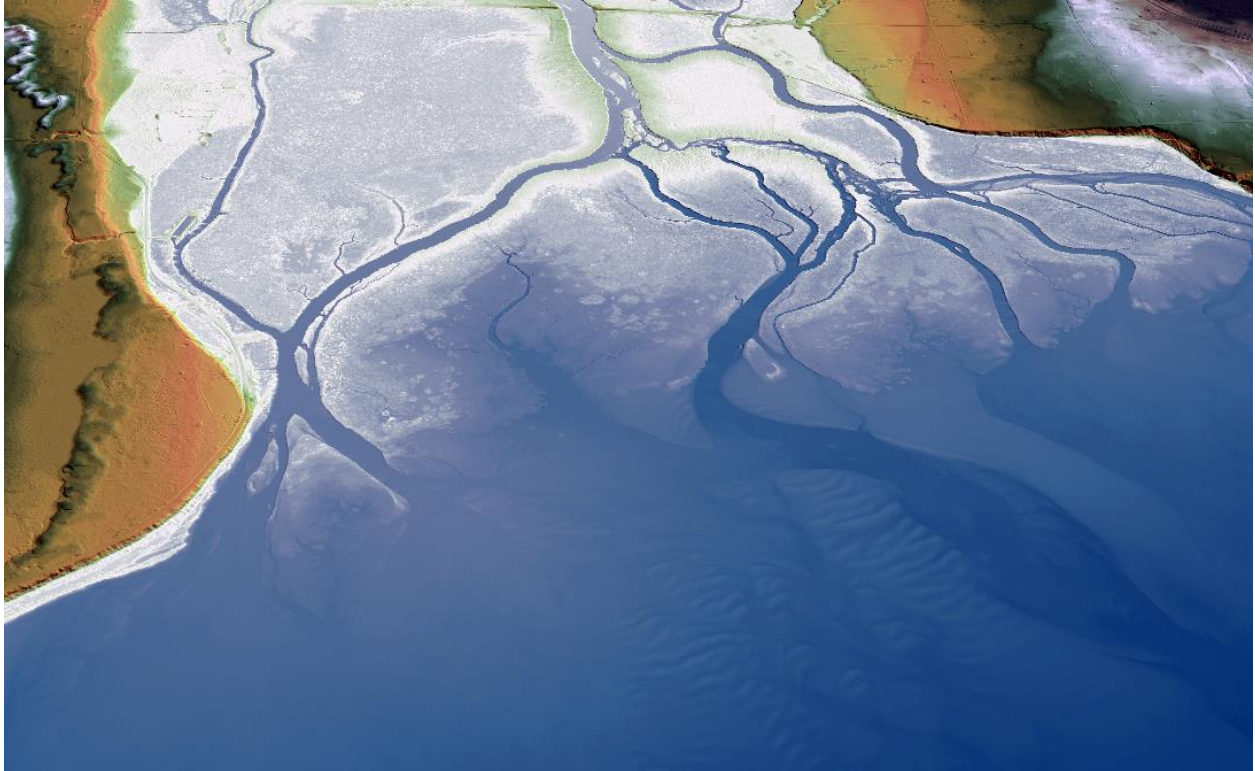


Figure 12: View looking north at the mouth of the Nooksack River at Bellingham Bay. Top image created from bare-earth LiDAR model colored by elevation. Bottom image created from the LiDAR point cloud with RGB values assigned by 2011 NAIP imagery.

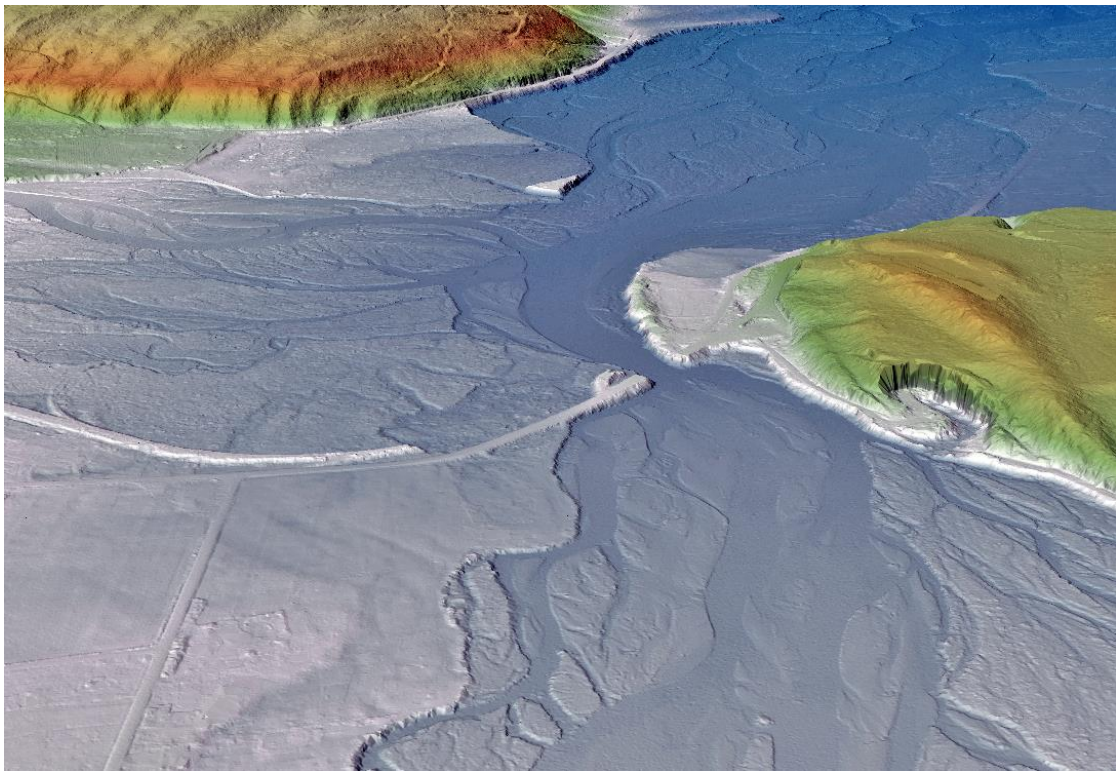


Figure 13: View looking south at the confluence of the North Fork and Middle Fork Nooksack Rivers near Welcome, Washington. The Mosquito Lake Road Bridge can be seen in the middle ground. Top image created from bare-earth LiDAR model colored by elevation. Bottom image created from the LiDAR point cloud with RGB values assigned by 2011 NAIP imagery.



Figure 14: Top image is a zoom view looking southwest up the Middle Fork Nooksack River towards the confluence with the North Fork Nooksack. Bottom image is a zoom view looking northeast up the North-Fork near Welcome, WA. Images created from the LiDAR point cloud with RGB values assigned by 2011 NAIP imagery.

1-sigma (σ) Absolute Deviation: Value for which the data are within one standard deviation (approximately 68th percentile) of a normally distributed data set.

1.96-sigma (σ) Absolute Deviation: Value for which the data are within two standard deviations (approximately 95th percentile) of a normally distributed data set.

Accuracy: The statistical comparison between known (surveyed) points and laser points, typically measured as the standard deviation (σ) and root mean square error (RMSE).

Absolute Accuracy: The vertical accuracy of LiDAR data is described as the mean and standard deviation (σ) of divergence of LiDAR point coordinates from RTK ground survey point coordinates. To provide a sense of the model predictive power of the dataset, the root mean square error (RMSE) for vertical accuracy is also provided. These statistics assume the error distributions for x, y, and z are normally distributed, thus we also consider the skew and kurtosis of distributions when evaluating error statistics.

Relative Accuracy: Relative accuracy refers to the internal consistency of the data set - the ability to place a laser point in the same location over multiple flight lines, GPS conditions, and aircraft attitudes. Affected by system attitude offsets, scale, and GPS/IMU drift, internal consistency is measured as the divergence between points from different flight lines within an overlapping area. Divergence is most apparent when flight lines are opposing. When the LiDAR system is well calibrated, the line-to-line divergence is low (<10 cm).

Root Mean Square Error (RMSE): A statistic used to approximate the difference between real-world points and the LiDAR points. It is calculated by squaring all the values, then taking the average of the squares and taking the square root of the average.

Data Density: A common measure of LiDAR resolution, measured as points per square meter.

DTM / DEM: These often-interchanged terms refer to models made from laser points. The digital elevation model (DEM) refers to all surfaces, including bare ground and vegetation, while the digital terrain model (DTM) refers only to those points classified as ground.

Intensity Values: The peak power ratio of the laser return to the emitted laser. It is a function of surface reflectivity.

Laser Noise: For any given target, laser noise is the breadth of the data cloud per laser return (i.e., last, first, etc.). Lower intensity surfaces (roads, rooftops, still/calm water) experience higher laser noise.

Nadir: A single point or locus of points on the surface of the earth directly below a sensor as it progresses along its flight line.

Overlap: The area shared between flight lines, typically measured in percent; 100% overlap is essential to ensure complete coverage and reduce laser shadows.

Pulse Rate (PR): The rate at which laser pulses are emitted from the sensor; typically measured as thousands of pulses per second (kHz).

Pulse Returns: For every laser pulse emitted, the Leica ALS 60 system can record *up to four* wave forms reflected back to the sensor. Portions of the wave form that return earliest are the highest element in multi-tiered surfaces such as vegetation. Portions of the wave form that return last are the lowest element in multi-tiered surfaces.

Real-Time Kinematic (RTK) Survey: GPS surveying is conducted with a GPS base station deployed over a known monument with a radio connection to a GPS rover. Both the base station and rover receive differential GPS data and the baseline correction is solved between the two. This type of ground survey is accurate to 1.5 cm or less.

Scan Angle: The angle from nadir to the edge of the scan, measured in degrees. Laser point accuracy typically decreases as scan angles increase.

Spot Spacing: Also a measure of LiDAR resolution, measured as the average distance between laser points.

APPENDIX A - ACCURACY CONTROLS

Relative Accuracy Calibration Methodology:

Manual System Calibration: Calibration procedures for each mission require solving geometric relationships that relate measured swath-to-swath deviations to misalignments of system attitude parameters. Corrected scale, pitch, roll and heading offsets were calculated and applied to resolve misalignments. The raw divergence between lines was computed after the manual calibration was completed and reported for each survey area.

Automated Attitude Calibration: All data were tested and calibrated using TerraMatch automated sampling routines. Ground points were classified for each individual flight line and used for line-to-line testing. System misalignment offsets (pitch, roll and heading) and scale were solved for each individual mission and applied to respective mission datasets. The data from each mission were then blended when imported together to form the entire area of interest.

Automated Z Calibration: Ground points per line were used to calculate the vertical divergence between lines caused by vertical GPS drift. Automated Z calibration was the final step employed for relative accuracy calibration.

LiDAR accuracy error sources and solutions:

Type of Error	Source	Post Processing Solution
GPS (Static/Kinematic)	Long Base Lines	None
	Poor Satellite Constellation	None
	Poor Antenna Visibility	Reduce Visibility Mask
Relative Accuracy	Poor System Calibration	Recalibrate IMU and sensor offsets/settings
	Inaccurate System	None
Laser Noise	Poor Laser Timing	None
	Poor Laser Reception	None
	Poor Laser Power	None
	Irregular Laser Shape	None

Operational measures taken to improve relative accuracy:

Low Flight Altitude: Terrain following is employed to maintain a constant above ground level (AGL). Laser horizontal errors are a function of flight altitude above ground (i.e., $\sim 1/3000^{\text{th}}$ AGL flight altitude).

Focus Laser Power at narrow beam footprint: A laser return must be received by the system above a power threshold to accurately record a measurement. The strength of the laser return is a function of laser emission power, laser footprint, flight altitude and the reflectivity of the target. While surface reflectivity cannot be controlled, laser power can be increased and low flight altitudes can be maintained.

Reduced Scan Angle: Edge-of-scan data can become inaccurate. The scan angle was reduced to a maximum of $\pm 15^\circ$ from nadir, creating a narrow swath width and greatly reducing laser shadows from trees and buildings.

Quality GPS: Flights took place during optimal GPS conditions (e.g., 6 or more satellites and PDOP [Position Dilution of Precision] less than 3.0). Before each flight, the PDOP was determined for the survey day. During all flight times, a dual frequency DGPS base station recording at 1-second epochs was utilized and a maximum baseline length between the aircraft and the control points was less than 19 km (11.5 miles) at all times.

Ground Survey: Ground survey point accuracy (i.e. <1.5 cm RMSE) occurs during optimal PDOP ranges and targets a minimal baseline distance of 4 miles between GPS rover and base. Robust statistics are, in part, a function of sample size (n) and distribution. Ground survey RTK points are distributed to the extent possible throughout multiple flight lines and across the survey area.

50% Side-Lap (100% Overlap): Overlapping areas are optimized for relative accuracy testing. Laser shadowing is minimized to help increase target acquisition from multiple scan angles. Ideally, with a 50% side-lap, the most nadir portion of one flight line coincides with the edge (least nadir) portion of overlapping flight lines. A minimum of 50% side-lap with terrain-followed acquisition prevents data gaps.

Opposing Flight Lines: All overlapping flight lines are opposing. Pitch, roll and heading errors are amplified by a factor of two relative to the adjacent flight line(s), making misalignments easier to detect and resolve.